

Large stable oscillations in amplitude dynamics of colliding soliton sequences

Avner Peleg¹, and Debananda Chakraborty²

¹ *Department of Exact Sciences, Afeka College of Engineering, Tel Aviv 69988, Israel and*

² *Department of Mathematics, New Jersey City University,*

Jersey City, New Jersey 07305, USA

(Dated: December 9, 2024)

Abstract

We demonstrate that the amplitudes of optical solitons in nonlinear multisequence optical waveguide coupler systems with linear and cubic gain-loss exhibit large stable oscillations along ultra-long distances. The large stable oscillations are caused by supercritical Hopf bifurcations of the equilibrium states of the Lotka-Volterra (LV) models for dynamics of soliton amplitudes. The predictions of the LV models are confirmed by simulations with the full coupled nonlinear Schrödinger propagation models for $2 \leq N \leq 4$ sequences. Our findings are an important step towards realizing spatio-temporal chaos with multiple sequences of colliding solitons in nonlinear optical waveguides.

PACS numbers: 42.65.Tg, 42.65.Sf, 05.45.Yv

Introduction. Nonlinear oscillations, i.e., oscillations with relatively large amplitudes, which are described by nonlinear dynamical models, appear in a wide range of systems, including mechanical oscillators [1, 2], electric circuits [2], chemical reactions [3, 4], and biological systems [4]. The occurrence and stability of such nonlinear oscillators is very often associated with the existence of a stable periodic attractor, i.e., a limit cycle, for the corresponding dynamical model. In many physical systems, the emergence of the stable limit cycle is due to a supercritical Hopf bifurcation [1–4]. In this case, as the value of a physical parameter is changed beyond some threshold value, a stable equilibrium state of the dynamical model becomes unstable, and a stable limit cycle about the unstable equilibrium state appears [1, 2]. Supercritical Hopf bifurcations are known to occur in many physical systems, including electric circuits [2], chemical reactions [3–5], and population dynamics [4, 6–8]. In the current study, we are interested in Lotka-Volterra models, which are known to describe dynamics of population sizes [9, 10] as well as the time evolution of chemical concentrations in certain chemical reactions [3–5]. The occurrence of supercritical Hopf bifurcations in LV models is of special interest, since in some cases, as the value of the bifurcation parameter is further changed, the limit cycle undergoes a period doubling cascade, and finally, chaotic dynamics is observed [5, 7, 8].

In the current paper, we study multisequence transmission of optical solitons in nonlinear waveguide systems with linear and cubic gain-loss. In this case, the solitons in each sequence propagate with the same frequency and group velocity, but the frequency and group velocity are different for solitons from different sequences [11]. As a result, intersequence soliton collisions are frequent and can lead to transmission degradation and significant amplitude shifts. In Refs. [12, 13], we showed that dynamics of soliton amplitudes in N -sequence nonlinear waveguide systems can be described by N -dimensional LV models. Furthermore, we showed that stability analysis of the equilibrium states of the LV models can be used for realizing transmission stabilization and switching [12, 13]. However, the results of these studies were limited to weakly nonlinear amplitude dynamics. The main obstacle for observing intermediate and strongly nonlinear amplitude dynamics is due to the instability of multisequence transmission of conventional optical solitons against resonant emission of small-amplitude waves [13, 14]. Therefore, intermediate or strongly nonlinear amplitude dynamics has not yet been observed in multisequence transmission with conventional optical solitons, or in any other physical system with cubic nonlinearity and multiple sequences of colliding solitons.

In the current paper, we demonstrate that the amplitudes of conventional optical solitons in multisequence nonlinear waveguide coupler systems with linear and cubic gain-loss can exhibit intermediate nonlinear dynamics. For this purpose, we show that supercritical Hopf bifurcations of the equilibrium states of the LV models for amplitude dynamics can be used to induce large stable oscillations of soliton amplitudes. The dynamics is realized despite of the inherent instability of multichannel transmission with conventional solitons. We validate the predictions of the LV models by numerical simulations with the full coupled nonlinear Schrödinger (NLS) propagation models for $2 \leq N \leq 4$ sequences. Since two of the LV models that we study exhibit chaotic dynamics, our findings are an important step towards realizing spatio-temporal chaos with multiple sequences of colliding solitons in nonlinear optical waveguides.

Propagation models. We consider propagation of N sequences of optical pulses in an optical waveguide coupler, consisting of N close waveguides, where each sequence propagates through its own waveguide. We assume a multisequence setup, where the pulses in each sequence propagate with the same group velocity, but where the group velocity is different for pulses from different sequences [11]. Additionally, we assume that the sequences propagate in the presence of second-order dispersion, Kerr nonlinearity, and weak linear and cubic gain-loss. Under these assumptions, propagation is described by the system of N coupled-NLS equations [11, 12, 14, 15]:

$$\begin{aligned}
i\partial_z\psi_j + \partial_t^2\psi_j + 2|\psi_j|^2\psi_j &= i\mathcal{F}^{-1}(G_j(\omega, z)\hat{\psi}_j)/2 \\
-2i\sum_{k=1}^N(1 - \delta_{jk})\epsilon_{3jk}|\psi_k|^2\psi_j, & \quad (1)
\end{aligned}$$

where ψ_j is the envelope of the electric field of the j th sequence, $1 \leq j \leq N$, z is propagation distance, t is time, and ω is frequency [16]. In Eq. (1), $G_j(\omega, z)$ is the linear gain-loss experienced by j th sequence pulses, $\hat{\psi}_j$ is the Fourier transform of ψ_j with respect to time, \mathcal{F}^{-1} is the inverse Fourier transform, and δ_{jk} is the Kronecker delta function. The coefficients ϵ_{3jk} describe the strength of cubic gain-loss interaction between j th and k th sequence pulses. The second and third terms on the left hand side of Eq. (1) describe second-order dispersion effects and intrasequence interaction due to Kerr nonlinearity. The first term on the right hand side of Eq. (1) describes the effects of frequency dependent linear gain-loss, while the second term corresponds to intersequence interaction due to cubic gain-loss. We assume that Kerr nonlinearity is narrowband, i.e., that it is negligible for frequency differences that

are much larger than the spectral width of the pulses. In addition, we assume that cubic gain-loss is broadband, i.e., that it is non-negligible only for frequency differences that are much larger than the spectral width of the pulses. As a result, we can neglect interchannel interaction due to Kerr nonlinearity and intrachannel interaction due to cubic gain-loss. These assumptions lead to significant enhancement of transmission stability and enable the observation of large stable oscillations of pulse amplitudes in simulations with Eq. (1).

The optical pulses in the j th sequence are fundamental solitons of the unperturbed NLS equation $i\partial_z\psi_j + \partial_t^2\psi_j + 2|\psi_j|^2\psi_j = 0$. The envelopes of these solitons are given by $\psi_{s_j}(t, z) = \eta_j \exp(i\chi_j)\text{sech}(x_j)$, where $x_j = \eta_j(t - y_j - 2\beta_j z)$, $\chi_j = \alpha_j + \beta_j(t - y_j) + (\eta_j^2 - \beta_j^2)z$, and η_j , β_j , y_j , and α_j are the soliton amplitude, frequency, position, and phase.

The form of the frequency dependent linear gain-loss function $G_j(\omega, z)$ is chosen such that the transmission is stabilized against radiation emission effects and collision-induced amplitude shifts due to cubic gain-loss. In particular, we choose the form [13, 14]: $G_j(\omega, z) = \epsilon_1 g_j(z)$ if $\beta_j(0) - W/2 < \omega \leq \beta_j(0) + W/2$ for $1 \leq j \leq N$, and $G_j(\omega, z) = -g_L$ elsewhere. Here ϵ_1 is the linear gain-loss coefficient, $\beta_j(0)$ is the initial frequency of j th sequence solitons, and $g_L > 0$. The spectral width W satisfies $1 < W \leq \Delta\beta$, where $\Delta\beta$ is the frequency spacing. The function $g_j(z)$ is: $g_j(z) = g_{1j} + g_{2j}\eta_j(z) + g_{3j}\eta_j^2(z)$, where $\eta_j(z)$ is the amplitude of j th sequence solitons. The values of the constants g_{1j} , g_{2j} , and g_{3j} are chosen such that collision-induced amplitude shifts due to cubic gain-loss are balanced by amplitude shifts due to linear gain-loss. This choice is guided by analysis of the LV model for amplitude dynamics. The values of g_L and W are chosen such that instability due to radiation emission is mitigated.

LV models for amplitude dynamics. In Refs. [12, 13], we showed that amplitude dynamics of N sequences of colliding solitons in the presence of weak dissipative perturbations can be described by N -dimensional LV models. The derivation of the LV models was based on the following assumptions. (1) The intrasequence separation T between adjacent solitons satisfies: $T \gg 1$. In addition, the amplitudes are equal for all solitons from the same sequence, but are not necessarily equal for solitons from different sequences. (2) The pulses circulate in a closed waveguide loop. (3) As $T \gg 1$, intrasequence interaction is exponentially weak and is neglected. (4) High-order radiation emission effects are also neglected.

Under these assumptions, the amplitudes of all pulses in a given sequence follow the same dynamics. Taking into account collision-induced amplitude shifts due to cubic gain-loss and single-pulse amplitude changes due to linear gain-loss, we obtain the following equation for

amplitude dynamics of j th sequence solitons [12]:

$$\frac{d\eta_j}{dz} = \eta_j \left[\epsilon_1 g_j(z) - \frac{8}{T} \sum_{k=1}^N (1 - \delta_{jk}) \epsilon_{3jk} \eta_k \right]. \quad (2)$$

Note that Eq. (2) has the form of a LV model for N species [9, 10]. The choice of physical parameter values in Eq. (2) is guided by the following requirements. (a) The LV model (2) has an equilibrium state with equal or near-equal amplitudes, as the value of the bifurcation parameter μ changes through 1. (b) The equilibrium state with near-equal amplitudes undergoes a supercritical Hopf bifurcation as μ changes through 1. As a result, the equilibrium state changes from a stable focus to an unstable state and a stable limit cycle around the unstable state appears. The emergence of the limit cycle is the key factor in enabling large stable oscillations of soliton amplitudes. Requirement (a) for near-equal amplitude values of the equilibrium state is added so that the perturbation procedure leading to the LV model is valid when μ is close to 1, i.e., near the Hopf bifurcation.

N-sequence transmission. We now consider three multisequence waveguide coupler transmission systems with linear and cubic gain-loss as prototypical examples for waveguide systems, where dynamics of soliton amplitudes with large stable oscillations that is induced by a Hopf bifurcation can be observed. For each transmission system, we present the predictions of the LV model (2), the results of simulations with the coupled-NLS model (1), and a comparison between the LV and coupled-NLS models.

The coupled-NLS system (1) is numerically solved using the split-step method with periodic boundary conditions [11], and thus the simulations describe propagation in a closed waveguide loop. The initial condition consists of N periodic sequences of $2K+1$ solitons with amplitudes $\eta_j(0)$, frequencies $\beta_j(0)$, and zero phases: $\psi_j(t, 0) = \sum_{k=-K}^K \eta_j(0) \exp[i\beta_j(0)(t - kT)] \operatorname{sech}[(\eta_j(0)(t - kT))]$, where $1 \leq j \leq N$, and $2 \leq N \leq 4$. To maximize transmission stability, we use $W = 10$ and $g_L = 0.5$ for the parameters of $G_j(\omega, z)$. We present the results of simulations with $T = 20$, $\Delta\beta = 40$, $K = 1$, and a final distance $z_f = 5000$. We emphasize that similar results are obtained with other physical parameter values.

Two-sequence transmission. The two-dimensional (2D) LV model for two-sequence transmission is a variant of the predator-prey model analyzed by Odell in Ref. [6]. The model is given by Eq. (2) with $N = 2$, $g_{11} = -\mu$, $g_{21} = g_{31} = 0$, $g_{12} = -1$, $g_{22} = 4$, $g_{32} = -2$, $\epsilon_{312} = -\epsilon_1 T/8$, $\epsilon_{321} = \epsilon_1 T/8$, where μ is a bifurcation parameter. Thus, the $j = 1$ sequence propagates in the presence of linear loss with coefficient $g_1 = -\mu$ and cubic gain intersequence

interaction, while the $j = 2$ sequence propagates in the presence of linear gain-loss with coefficient $g_2(z) = -1 + 4\eta_j - 2\eta_j^2$ and cubic loss intersequence interaction. The equilibrium state with near-equal amplitudes is $(\eta_1^{(eq)}, \eta_2^{(eq)}) = (-1 + 4\mu - 2\mu^2, \mu)$. This state undergoes a supercritical Hopf bifurcation as μ changes through 1. For $\mu < 1$, the equilibrium state is an unstable focus, which is surrounded by a stable limit cycle, while for $\mu > 1$, it is a stable focus and the limit cycle does not exist [6]. Thus, we expect large stable amplitude oscillations for $\mu < 1$, and stable oscillations that decay to $\eta_j^{(eq)}$ for $\mu > 1$. To test these predictions, we numerically solve Eq. (1) with $\epsilon_1 = 0.05$ for different μ values close to 1. Figure 1 shows the z dependence of η_j obtained by the simulations for $\mu = 0.98$ with $\eta_1(0) = 0.95$ and $\eta_2(0) = 1.05$ together with the LV model's predictions. It is seen that the amplitudes exhibit large stable oscillations that approach limit cycle behavior, in very good agreement with the LV model's predictions. Additionally, as seen in Fig. 4 (Supplemental Fig. 1), for $\mu = 1.05$, the amplitudes exhibit decaying oscillations and approach their equilibrium values $\eta_j^{(eq)}$. Furthermore, in both cases the solitons retain their shape throughout the propagation [see Fig. 5 (Supplemental Fig. 2)]. Similar results are obtained for other values of μ and the $\eta_j(0)$.

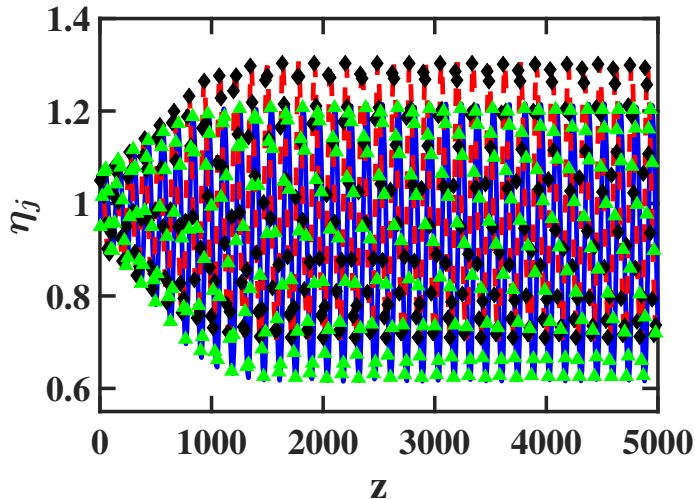


FIG. 1: (Color online) The z -dependence of soliton amplitudes η_j in two-sequence transmission for $\mu = 0.98$. The solid blue and dashed red curves represent $\eta_j(z)$ with $j = 1, 2$, obtained with Eq. (1). The black diamonds and green triangles represent $\eta_j(z)$ with $j = 1, 2$, obtained by the LV model (2).

Three-sequence transmission. The 3D LV model for amplitude dynamics in three-sequence transmission was studied by Arneodo et al. in Ref. [7]. The model is given by Eq. (2) with $N = 3$, $g_{11} = 1.1$, $g_{21} = -0.5$, $g_{12} = -0.5$, $g_{22} = 0.1$, $g_{13} = 0.2 + \mu$, $g_{23} = -0.1$, $g_{31} = g_{32} = g_{33} = 0$, $\epsilon_{312} = 0.5\epsilon_1 T/8$, $\epsilon_{313} = 0.1\epsilon_1 T/8$, $\epsilon_{321} = -0.5\epsilon_1 T/8$, $\epsilon_{323} = 0.1\epsilon_1 T/8$, $\epsilon_{331} = \mu\epsilon_1 T/8$, $\epsilon_{332} = 0.1\epsilon_1 T/8$. The relevant equilibrium state is $(1, 1, 1)$, independent of the value of μ [7]. This equilibrium state undergoes a supercritical Hopf bifurcation as μ increases through $\mu_H \simeq 0.954$ [7]. As a result, for $\mu < \mu_H$, the equilibrium state is a stable focus, while for $\mu > \mu_H$, $(1, 1, 1)$ becomes unstable and a stable limit cycle about $(1, 1, 1)$ appears. As μ increases beyond $\mu_P \simeq 1.265$, the limit cycle undergoes a period doubling cascade, and finally, chaotic dynamics is observed [7]. Thus, we expect to observe stable amplitude oscillations that decay to 1 for $\mu < \mu_H$, and large stable amplitude oscillations with a single period for $\mu_H < \mu < \mu_P$. To validate these predictions, we numerically solve Eq. (1) with $\epsilon_1 = 0.1$ for different μ values. Figure 2 shows the $\eta_j(z)$ dynamics obtained by the simulations for $\mu = 0.98$ with $\eta_1(0) = 0.95$, $\eta_2(0) = 1.05$, and $\eta_3(0) = 1.2$ together with the LV model's predictions. We observe that the amplitudes exhibit large stable oscillations that tend to limit cycle behavior, in very good agreement with the LV model's predictions. Additionally, as seen in Fig. 6 (Supplemental Fig. 3), for $\mu = 0.85$, the amplitudes exhibit decaying oscillations and approach their equilibrium value of 1. Furthermore, in both cases the soliton patterns remain intact throughout the propagation [see Fig. 7 (Supplemental Fig. 4)].

Four-sequence transmission. The 4D LV model for four-sequence transmission was studied in Ref. [8] by Arneodo et al. This LV model is given by Eq. (2) with $N = 4$, $g_{1j} = 3.3$ for $j = 1, 2, 3, 4$, $g_{21} = -1$, $g_{22} = -0.4$, $g_{23} = -0.6$, $g_{24} = -1.8$, $g_{3j} = 0$ for $j = 1, 2, 3, 4$, $\epsilon_{312} = \epsilon_1 T/8$, $\epsilon_{313} = 0.6\epsilon_1 T/8$, $\epsilon_{314} = 0.7\epsilon_1 T/8$, $\epsilon_{321} = 0$, $\epsilon_{323} = 0.6\epsilon_1 T/8$, $\epsilon_{324} = 2.3\epsilon_1 T/8$, $\epsilon_{331} = (\mu + 0.5)\epsilon_1 T/8$, $\epsilon_{332} = 0.6\epsilon_1 T/8$, $\epsilon_{334} = (1.6 - \mu)\epsilon_1 T/8$, and $\epsilon_{34j} = 0.5\epsilon_1 T/8$ for $j = 1, 2, 3, 4$. Note that all soliton sequences propagate in the presence of cubic loss intersequence interaction. This is very different from the two-sequence and three-sequence systems considered above, where one of the soliton sequences propagated in the presence of cubic gain interaction. The 4D LV model of Ref. [8] is in fact equivalent to the 3D LV model of Ref. [7]. Therefore, the relevant equilibrium state for amplitude dynamics is $(1, 1, 1, 1)$. This equilibrium state undergoes a supercritical Hopf bifurcation at $\mu_H \simeq 0.954$ [8], and as a result, the state $(1, 1, 1, 1)$ turns from a stable focus to an unstable state and a limit cycle

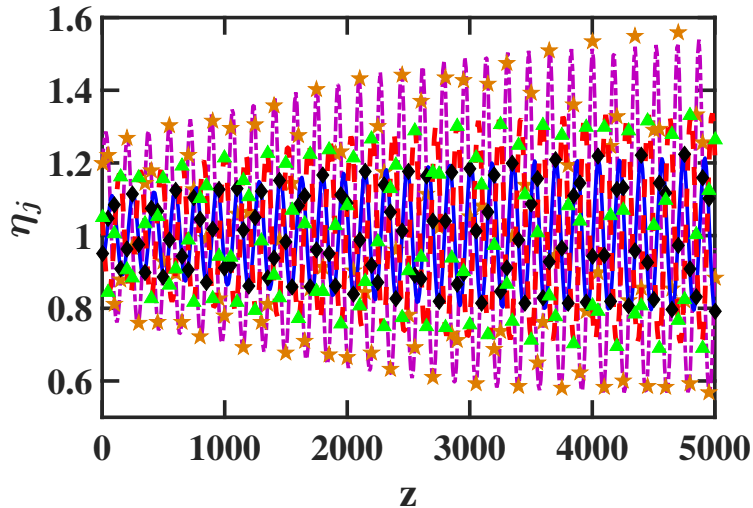


FIG. 2: (Color online) The z -dependence of soliton amplitudes η_j in three-sequence transmission for $\mu = 0.98$. The solid blue, dashed red, and dash-dotted purple curves represent $\eta_j(z)$ with $j = 1, 2, 3$, obtained by simulations with Eq. (1). The black diamonds, green triangles, and orange stars represent $\eta_j(z)$ with $j = 1, 2, 3$, obtained by the LV model (2).

about $(1, 1, 1, 1)$ appears. As μ is increased beyond $\mu_P \simeq 1.265$, the limit cycle undergoes a period doubling cascade, and finally, chaotic dynamics is observed [8]. Thus, we expect to observe large stable amplitude oscillations with a single period for $\mu_H < \mu < \mu_P$. To check the predictions of the 4D LV model, we numerically solve Eq. (1) with $\epsilon_1 = 0.05$ for different μ values. The z dependence of soliton amplitudes obtained by the simulations with $\mu = 0.98$ and $\eta_1(0) = 0.9$, $\eta_2(0) = 1.2$, $\eta_3(0) = 0.95$, and $\eta_4(0) = 1.15$, is shown in Fig. 3 along with the LV model's predictions. We observe that the amplitudes exhibit large stable oscillations that tend to limit cycle behavior, in very good agreement with the LV model's predictions. Additionally, as seen in Fig. 8 (Supplemental Fig. 5), for $\mu = 0.85$, the amplitudes exhibit decaying oscillations and tend to their equilibrium value of 1. Furthermore, in both cases the soliton patterns remain intact throughout the propagation [see Fig. 9 (Supplemental Fig. 6)]. Similar results are obtained for other values of μ and the $\eta_j(0)$. Based on our findings, we conclude that large stable oscillations of soliton amplitudes can indeed be observed in N -sequence transmission with $2 \leq N \leq 4$.

Summary. We demonstrated that the amplitudes of optical solitons in multisequence waveguide coupler systems with linear and cubic gain-loss exhibit large stable oscillations

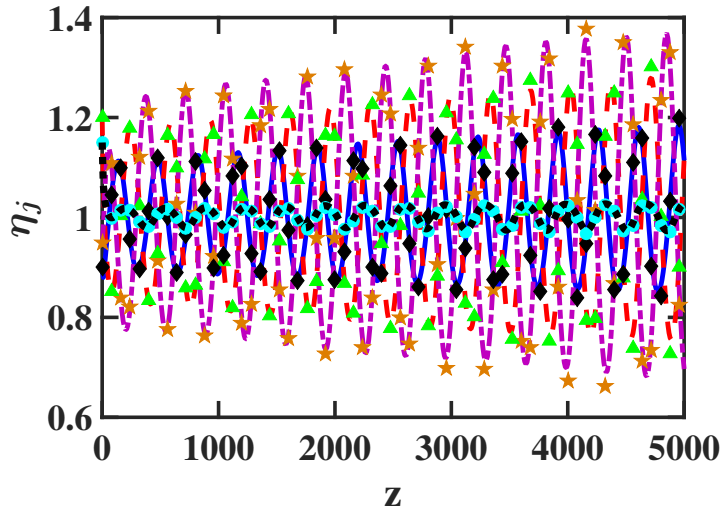


FIG. 3: (Color online) Soliton amplitudes η_j vs z in four-sequence transmission for $\mu = 0.98$. The solid blue, dashed red, dash-dotted purple, and dotted black curves represent $\eta_j(z)$ with $j = 1, 2, 3, 4$, obtained with Eq. (1). The black diamonds, green triangles, orange stars, and cyan circles represent $\eta_j(z)$ with $j = 1, 2, 3, 4$, obtained by the LV model (2).

along ultra-long distances. We showed that the stable oscillations are caused by Hopf bifurcations of the equilibrium states of the LV models for amplitude dynamics. The predictions of the LV models were confirmed by simulations with the coupled-NLS propagation models for $2 \leq N \leq 4$ sequences. Our results are very surprising, since multisequence transmission with conventional optical solitons is considered to be unstable against radiation emission. Moreover, since two of the LV models exhibit chaotic dynamics, our results are an important step towards realization of spatio-temporal chaos with multiple sequences of colliding optical solitons.

Supplemental Material

Here we provide supplemental figures of amplitude dynamics and pulse patterns at the final propagation distance for the three multichannel waveguide coupler transmission systems considered in our paper.

Supplemental figures for two-sequence transmission.

Figure 4 shows the z dependence of soliton amplitudes for two-sequence transmission

as obtained by numerical simulations with Eq. (1) with $\mu = 1.05$, $\epsilon_1 = 0.05$, and initial amplitudes $\eta_1(0) = 0.95$ and $\eta_2(0) = 1.05$. The prediction of the LV model (2) is also shown.

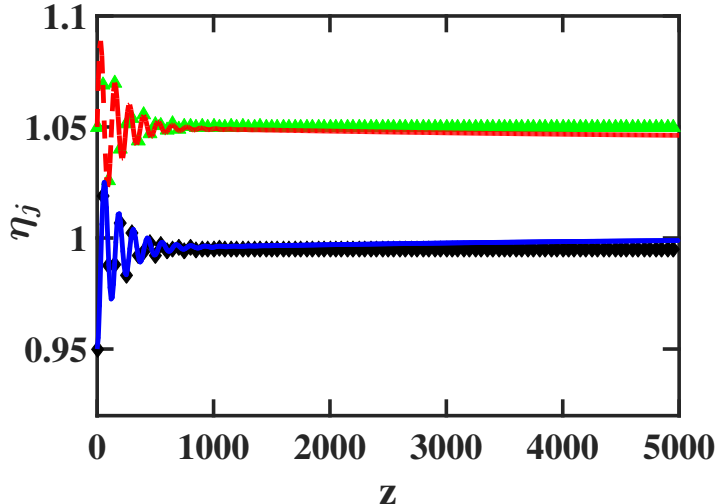


FIG. 4: (Color online) The z -dependence of soliton amplitudes η_j in two-sequence transmission for $\mu = 1.05$. The solid blue and dashed red curves represent $\eta_j(z)$ with $j = 1, 2$, obtained by simulations with Eq. (1). The black diamonds and green triangles represent $\eta_j(z)$ with $j = 1, 2$, obtained by the LV model (2).

Figure 5 shows the pulse patterns at the final propagation distance $|\psi_j(t, z_f)|$, where $z_f = 5000$, obtained by numerical simulations with Eq. (1) for two-sequence transmission with $\mu = 0.98$ (a) and $\mu = 1.05$ (b). The linear gain-loss coefficient is $\epsilon_1 = 0.05$ and the initial amplitudes are $\eta_1(0) = 0.95$ and $\eta_2(0) = 1.05$. The theoretical prediction, obtained by summation over fundamental NLS solitons, is also shown.

Supplemental figures for three-sequence transmission.

Figure 6 shows the z dependence of soliton amplitudes for three-sequence transmission as obtained by numerical simulations with Eq. (1) with $\mu = 0.85$ and $\epsilon_1 = 0.1$. The initial amplitudes are $\eta_1(0) = 0.95$, $\eta_2(0) = 1.05$, and $\eta_3(0) = 1.2$. The prediction of the LV model (2) is also shown.

Figure 7 shows the pulse patterns at the final propagation distance $|\psi_j(t, z_f)|$, where $z_f = 5000$, obtained by numerical simulations with Eq. (1) for three-sequence transmission with $\mu = 0.85$ (a) and $\mu = 0.98$ (b). The linear gain-loss coefficient is $\epsilon_1 = 0.1$ and the initial

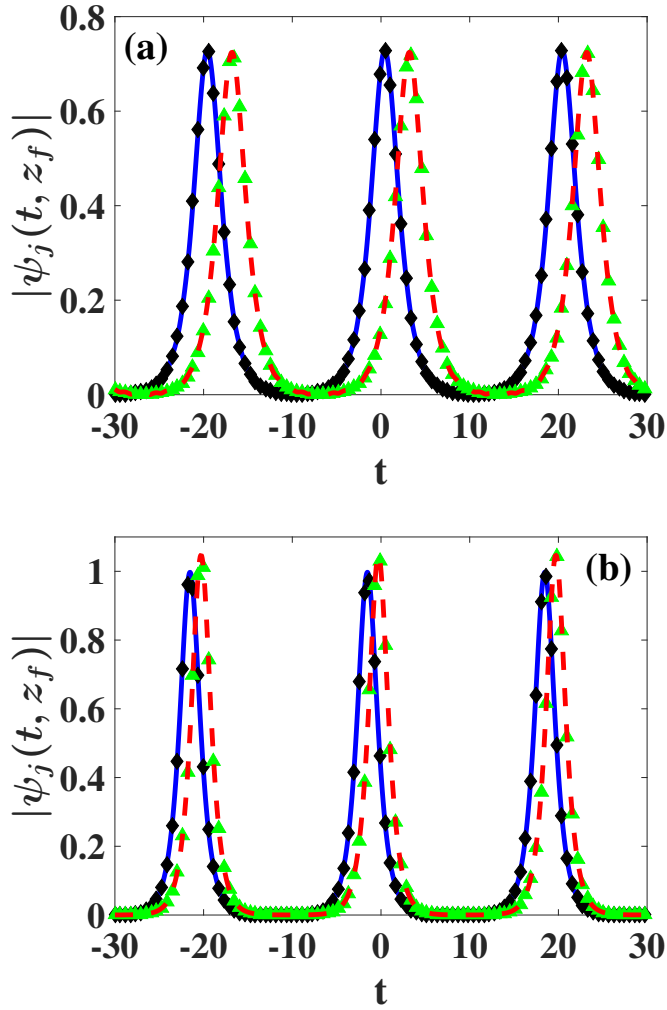


FIG. 5: (Color online) The pulse patterns at the final propagation distance $|\psi_j(t, z_f)|$, where $z_f = 5000$, for two-sequence transmission with $\mu = 0.98$ (a) and $\mu = 1.05$ (b). The linear gain-loss coefficient is $\epsilon_1 = 0.05$ and the initial amplitudes are $\eta_1(0) = 0.95$ and $\eta_2(0) = 1.05$. The solid blue and dashed red curves correspond to $|\psi_j(t, z_f)|$ with $j = 1, 2$, obtained by simulations with Eq. (1). The black diamonds and green triangles correspond to the theoretical prediction.

amplitudes are $\eta_1(0) = 0.95$, $\eta_2(0) = 1.05$, and $\eta_3(0) = 1.2$. The theoretical prediction, obtained by summation over fundamental NLS solitons, is also shown.

Supplemental figures for four-sequence transmission.

Figure 8 shows the z dependence of soliton amplitudes for four-sequence transmission as obtained by numerical simulations with Eq. (1) with $\mu = 0.85$ and $\epsilon_1 = 0.05$. The initial amplitudes are $\eta_1(0) = 0.9$, $\eta_2(0) = 1.2$, $\eta_3(0) = 0.95$, and $\eta_4(0) = 1.15$. The prediction of

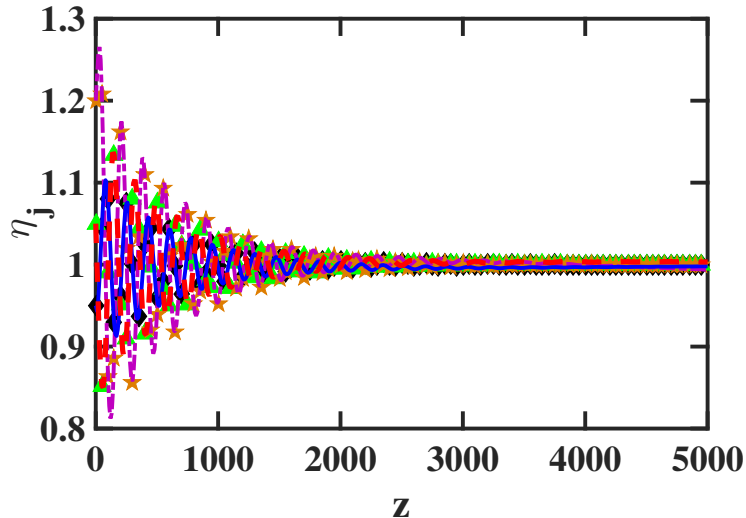


FIG. 6: (Color online) The z -dependence of soliton amplitudes η_j in three-sequence transmission for $\mu = 0.85$. The solid blue, dashed red, and dash-dotted purple curves represent $\eta_j(z)$ with $j = 1, 2, 3$, obtained by simulations with Eq. (1). The black diamonds, green triangles, and orange stars represent $\eta_j(z)$ with $j = 1, 2, 3$, obtained by the LV model (2).

the LV model (2) is also shown.

Figure 9 shows the pulse patterns at the final propagation distance $|\psi_j(t, z_f)|$, where $z_f = 5000$, obtained by numerical simulations with Eq. (1) for four-sequence transmission with $\mu = 0.85$ (a) and $\mu = 0.98$ (b). The linear gain-loss coefficient is $\epsilon_1 = 0.05$ and the initial amplitudes are $\eta_1(0) = 0.9$, $\eta_2(0) = 1.2$, $\eta_3(0) = 0.95$, and $\eta_4(0) = 1.15$. The theoretical prediction, obtained by summation over fundamental NLS solitons, is also shown.

-
- [1] J. Guckenheimer and P.J. Holmes, *Nonlinear Oscillations, Dynamical Systems, and Bifurcations of Vector Fields* (Springer, New York, 1983).
 - [2] M. Lakshmanan and S. Rajasekar, *Nonlinear Dynamics* (Springer, Berlin, 2002).
 - [3] R.J. Field and M. Burger, eds., *Oscillations and Traveling Waves in Chemical Systems* (Wiley, New York, 1985).
 - [4] J.D. Murray, *Mathematical Biology* (Springer, New York, 1989).
 - [5] E. Di Cera, P.E. Phillipson, and J. Wyman, Proc. Natl. Acad. Sci. USA **86**, 142 (1989).

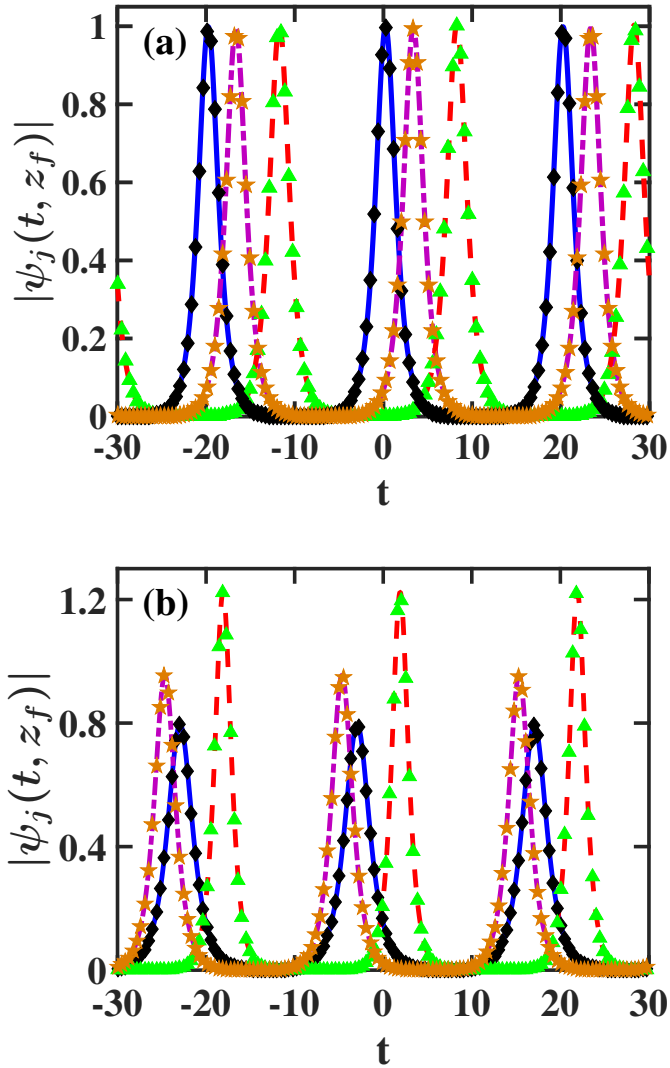


FIG. 7: (Color online) The pulse patterns at the final propagation distance $|\psi_j(t, z_f)|$, where $z_f = 5000$, for three-sequence transmission with $\mu = 0.85$ (a) and $\mu = 0.98$ (b). The linear gain-loss coefficient is $\epsilon_1 = 0.1$ and the initial amplitudes are $\eta_1(0) = 0.95$, $\eta_2(0) = 1.05$, and $\eta_3(0) = 1.2$. The solid blue, dashed red, and dash-dotted purple curves correspond to $|\psi_j(t, z_f)|$ with $j = 1, 2, 3$, obtained by simulations with Eq. (1). The black diamonds, green triangles, and orange stars correspond to the theoretical prediction.

[6] M.G. Odell, in *Mathematical models in molecular and cellular biology*, edited by L.A. Segel (Cambridge University Press, Cambridge, England, 1980), Appendix A.3.

[7] A. Arneodo, P. Coulet, and C. Tresser, *Phys. Lett. A* **79**, 259 (1980).

[8] A. Arneodo et al., *J. Math. Biology* **14**, 153 (1982).

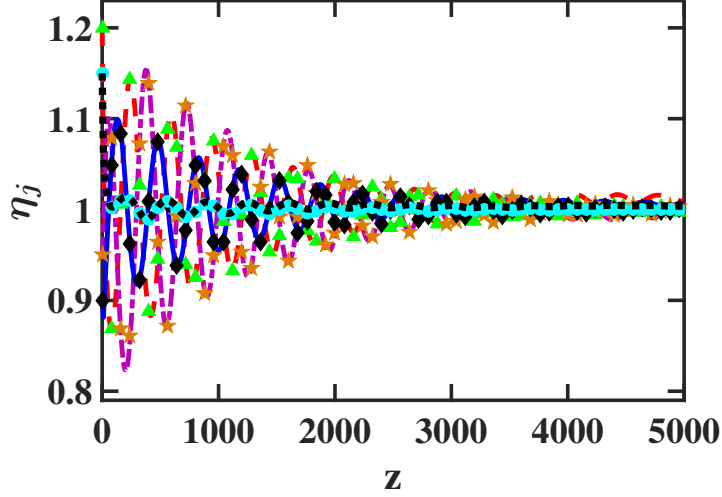


FIG. 8: (Color online) Soliton amplitudes η_j vs z in four-sequence transmission for $\mu = 0.85$. The solid blue, dashed red, dash-dotted purple, and dotted black curves represent $\eta_j(z)$ with $j = 1, 2, 3, 4$, obtained by simulations with Eq. (1). The black diamonds, green triangles, orange stars, and cyan circles represent $\eta_j(z)$ with $j = 1, 2, 3, 4$, obtained by the LV model (2).

- [9] A.J. Lotka, *Elements of Physical Biology* (Williams and Wilkins, Baltimore, 1925).
- [10] V. Volterra, *J. Cons. Int. Explor. Mer* **3**, 1 (1928).
- [11] G.P. Agrawal, *Nonlinear Fiber Optics* (Academic, San Diego, CA, 2001).
- [12] A. Peleg, Q.M. Nguyen, and Y. Chung, *Phys. Rev. A* **82**, 053830 (2010).
- [13] A. Peleg, Q.M. Nguyen, and T.P. Tran, *Opt. Commun.* **380**, 41 (2016).
- [14] D. Chakraborty, A. Peleg, and Q.M. Nguyen, *Opt. Commun.* **371**, 252 (2016).
- [15] Q. Lin, O.J. Painter, and G.P. Agrawal, *Opt. Express* **15**, 16604 (2007).
- [16] The dimensionless distance z in Eq. (1) is $z = X/(2L_D)$, where X is the dimensional distance, $L_D = \tau_0^2/|\tilde{\beta}_2|$ is the dispersion length, τ_0 is the soliton width, and $\tilde{\beta}_2$ is the second-order dispersion coefficient. The dimensionless time is $t = \tau/\tau_0$, where τ is time. $\psi_j = E_j/\sqrt{P_0}$, where E_j is the electric field of the j th sequence and P_0 is peak power. The dimensionless second-order dispersion coefficient is $d = -1 = \tilde{\beta}_2/(\gamma P_0 \tau_0^2)$, where γ is the Kerr nonlinearity coefficient. The coefficients ϵ_1 and ϵ_{3jk} are related to the dimensional linear and cubic gain-loss coefficients ρ_1 and ρ_{3jk} by $\epsilon_1 = 2\tau_0^2\rho_1/|\tilde{\beta}_2|$ and $\epsilon_{3jk} = 2\rho_{3jk}^{(1)}/\gamma$. The solitons spectral width is $\nu_0 = 1/(\pi^2\tau_0)$ and the intersequence frequency difference is $\Delta\nu = (\pi\Delta\beta\nu_0)/2$.

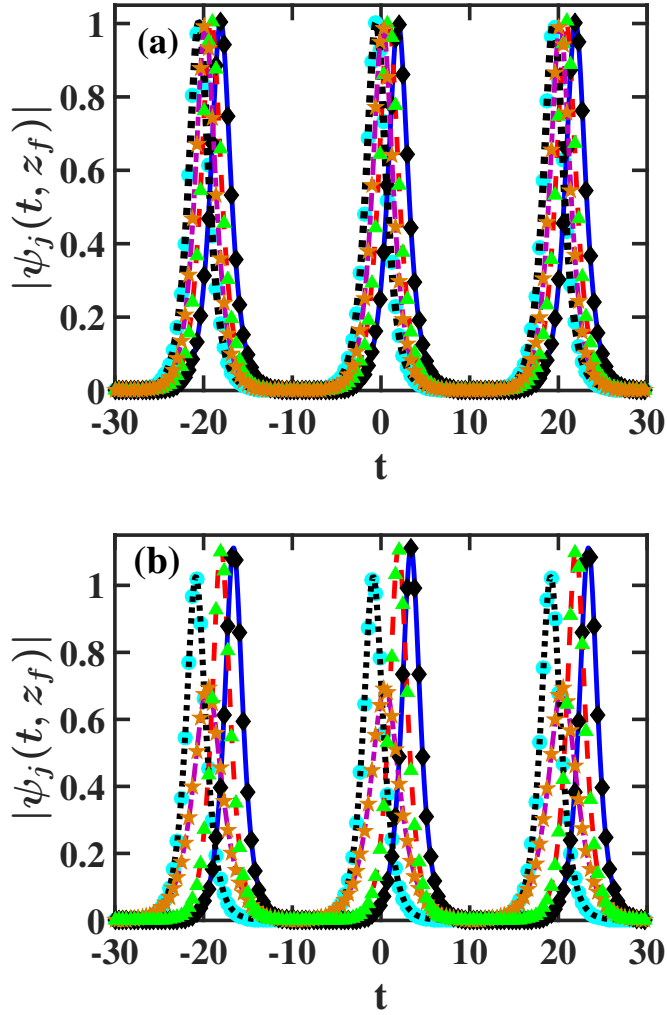


FIG. 9: (Color online) The pulse patterns at the final propagation distance $|\psi_j(t, z_f)|$, where $z_f = 5000$, for four-sequence transmission with $\mu = 0.85$ (a) and $\mu = 0.98$ (b). The linear gain-loss coefficient is $\epsilon_1 = 0.05$ and the initial amplitudes are $\eta_1(0) = 0.9$, $\eta_2(0) = 1.2$, $\eta_3(0) = 0.95$, and $\eta_4(0) = 1.15$. The solid blue, dashed red, dash-dotted purple, and dotted black curves correspond to $|\psi_j(t, z_f)|$ with $j = 1, 2, 3, 4$, obtained by simulations with Eq. (1). The black diamonds, green triangles, orange stars, and cyan circles correspond to the theoretical prediction.